Metabolic Control of Elastic Properties of the Inner Mitochondrial Membrane

Michael Chvanov*

Department of Physiology, The University of Liverpool, Crown Street, Liverpool L69 3BX, United Kingdom

Received: June 19, 2006; In Final Form: August 21, 2006

A possible physical mechanism for inner mitochondrial membrane shape rearrangements is given. This analytical study shows that high transmembrane potential at the inner mitochondrial membrane brings about specific, substantial, and dynamic electrochemical contributions to lateral tension, bending rigidity constant, and elastic modulus of Gaussian curvature of the membrane. Changes in mitochondrial metabolism dramatically affect the magnitude of these elastic parameters but not necessarily that of proton-motive force. Metabolic-driven variation of mechanical properties of the inner mitochondrial membrane can promote the membrane remodeling between its principal geometric shapes and serve as a negative feedback in control of the oxidative phosphorylation.

Introduction

Mitochondria are plastic organelles with complex and dynamic structure. In living cells they undergo continuous shape transformations, including isovolumic reshaping, fission/fusion rearrangements, and contraction−swelling volume changes. The shape of a biological membrane is created by molecular interactions between membrane lipids and proteins and by external physical forces applied to the membrane.[1,2] The structure of the membrane as a whole depends substantially on the bulk mechanical parameters of the membrane such as lateral tension, bending rigidity constant, elastic modulus of Gaussian curvature, and spontaneous curvature. For instance, cortical tension at the plasma membrane is a global factor that controls cell surface motility and regulates the balance between cellular exocytosis and endocytosis,[3−5] whereas minimum bending energy of the membrane determines the biconcave shape of erythrocytes.[6,7] Elastic properties of biological membranes, in turn, depend significantly on electrostatic interactions between the membrane and the ambient ions.[8,9] In the mitochondria much is known about the macromolecules regulating the structure and dynamics of the mitochondrial membranes;[10−13] however relation of macroscopic mechanical parameters and the mitochondrial shape has not been addressed yet. The aim of this study was to (i) obtain analytical expressions and numerical estimates for electrochemical contributions associated with proton-motive force to lateral tension, bending rigidity constant, and the elastic modulus of Gaussian curvature of the inner mitochondrial membrane under state 4 and state 3 respiration conditions and (ii) assess the physiological role of the mechanical properties of the inner mitochondrial membrane.

Results

1. Electrochemical Surface Tension. Consider the inner mitochondrial membrane as a parallel-plate electric capacitor. The capacitance C of the membrane is proportional to the area of the membrane surface S

$$C = \frac{\epsilon_m \epsilon_0}{2d} S = cS \tag{1}$$

where ϵ_0 and ϵ_m are the dielectric constants for free space and membrane respectively, $2d$ is the membrane thickness, and c is the capacitance per unit area. We assume d (and hence c) constant during changes of S. The proton-motive force Δp consists of membrane potential $\Delta\Psi$ and the pH gradient

$$\Delta p = \frac{\Delta\bar{\mu}_{H^+}}{F} = \Delta\Psi - \frac{RT}{F}\Delta\mathrm{pH} \tag{2}$$

and the free energy associated with the electric charge (Q) separated by the membrane reads

$$W_e = \int \Delta\bar{\mu}_{H^+}\, dn = \int \Delta\Psi\, dQ - \frac{RT}{F}\int \Delta\mathrm{pH}\, dQ = \frac{Q^2}{2C} - \frac{RT}{F}\int \Delta\mathrm{pH}\, dQ = \frac{1}{2}C(\Delta\Psi)^2 - \frac{RT}{F}\int \Delta\mathrm{pH}\, dQ \tag{3}$$

where n is the amount of protons in moles, $\Delta\mu_{H^+}$ is the electrochemical potential gradient for protons, and Q is equal to $cS\Delta\Psi$. Substituting C from eq 1, one obtains

$$W_e = \frac{Q^2}{2cS} - \frac{RT}{F}\int \Delta\mathrm{pH}\, dQ = \frac{1}{2}cS(\Delta\Psi)^2 - \frac{RT}{F}\int \Delta\mathrm{pH}\, dQ \tag{4}$$

Dependence between the electrochemical term of the membrane free energy and the surface area means that if the membrane shape is allowed to change its area, it will do so to minimize free energy. In this case nonzero surface curvature will create additional pressure analogous to interfacial pressure in liquids. The effective surface tension coefficient σ_e equals

$$\sigma_e = \frac{\partial W_e}{\partial S} \tag{5}$$

The magnitude of this coefficient depends on the speed of mitochondrial reshaping. If fluctuations in the membrane shape occur much faster than the rate by which mitochondria can compensate for $\Delta\Psi$ changes, then the energy variation in eq 5 occurs at effectively constant electric charge Q accumulated at the surfaces of the mitochondrial membrane. However, if the mitochondrial reshaping is slow, then one can consider $\Delta\Psi$ as

* Author to whom correspondence should be addressed. E-mail: chvanov@liv.ac.uk.

10.1021/jp0638181 CCC: $33.50
Published on Web 10/13/2006

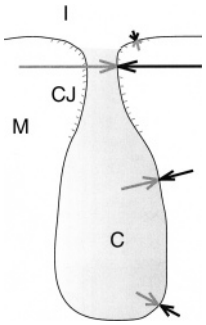

Figure 1. Schematic structure of a crista connection to the inner boundary membrane within the inner mitochondrial membrane. Black and gray arrows show the electrochemical surface pressure (P_e) forces under constant $\Delta\Psi$ and constant Q conditions, respectively (see the text); the hatches highlight the area of the membrane with negative Gaussian curvature: C, crista; M, matrix; I, intermembrane space; CJ, crista junction.

constant. Either of these two extremes (constancy of Q or constancy of $\Delta\Psi$) can take place in physiological conditions, as will be shown in section 3.

It seems reasonable to assume that mitochondrial reshaping itself (at any speed) does not affect matrix ΔpH so that when the surface varies by δS

$$\delta(\int \Delta\mathrm{pH}\, \mathrm{d}Q) = \Delta\mathrm{pH}\, \delta Q \tag{6}$$

Thus, in the case of constant $\Delta\Psi$, the effective electrochemical surface tension coefficient equals

$$\sigma_e = \left(\frac{\partial W_e}{\partial S}\right)_{\Delta\Psi} = \frac{1}{2}c(\Delta\Psi)^2 - \frac{RT}{F}c\Delta\mathrm{pH}\Delta\Psi \tag{7}$$

In this case the local pressure on the surface of the inner membrane, according to Laplace's formula, is equal to

$$P_e = \left\{\frac{1}{2}c(\Delta\Psi)^2 - \frac{RT}{F}c\Delta\mathrm{pH}\Delta\Psi\right\}\left(\frac{1}{R_1} + \frac{1}{R_2}\right) \tag{8}$$

where R_1 and R_2 denote principal radii of curvature of the membrane. The positive value of P_e reflects the fact that the flexible capacitor, whose potential is maintained constant, would minimize its potential energy by reducing the surface area and creating tension/pressure acting toward compression of the membrane and squeezing the bottleneck of the cristae junctions (Figure 1).

In the case of constant electric charge, the values for the electrochemical surface tension coefficient and surface pressure are

$$\sigma_e = \left(\frac{\partial W_e}{\partial S}\right)_Q = -\frac{1}{2}c(\Delta\Psi)^2 \tag{9}$$

and

$$P_e = -\frac{1}{2}c(\Delta\Psi)^2\left(\frac{1}{R_1} + \frac{1}{R_2}\right) \tag{10}$$

The negative sign for σ_e and P_e in eqs 9 and 10 means that when there is no resupply of the electric charge the additional electromechanical tension/pressure tends to expand the membrane and widen cristae junctions (Figure 1).

Using $\Delta\Psi \approx -0.16$ V, ΔpH ≈ 1, and $c \approx 3$ μF/cm^2, I obtained the estimates for the magnitude of the electrochemical surface tension coefficient as follows: $\sigma_e \approx 0.5$ mN/m in the constant $\Delta\Psi$ approximation and $\sigma_e \approx -0.38$ mN/m in the constant Q approximation. It is worth noting that the $c \approx 3$ μF/cm^2 value used is higher than the typical capacitance per unit area of the cellular plasma membrane (which is around 1 μF/cm^2). The value of c for the inner mitochondrial membrane was obtained from Figure 1 in ref 14, using data for the current amplitude in panel c of this figure, current density in panel d, and the mitoplast size in panel b.

According to the current view, the mitochondrial cristae regions are connected with the inner boundary membrane via cristae junctions.[15] In a number of mitochondrial preparations, the cristae exist as tubular protrusions of intermembrane space into the inner part of the mitochondria (shown schematically in Figure 1). The bottleneck of these protrusions has a standard diameter of approximately 27−30 nm and can be a limiting point for diffusion between intermembrane and intracristae spaces.[16,17] Using a 15 nm estimate for the radius of curvature and $c \approx 3$ μF/cm^2, one obtains the estimates for the local electromechanical surface pressure P_e at the cristae junctions of 3.3×10^4 and -2.5×10^4 Pa in the case of constant $\Delta\Psi$ and Q, respectively.

2. Electrochemical Components in the Bending Rigidity Constant and the Elastic Modulus of Gaussian Curvature. At small length scales (up to several tens of nanometers) bending elasticity becomes the key factor in control of the membrane shape.[7,18−20] The free energy of the membrane per unit area associated with bending reads

$$w_s = -kc_0(c_1 + c_2) + \frac{k}{2}(c_1 + c_2)^2 + k_G c_1 c_2 \tag{11}$$

where c_0 is spontaneous curvature, c_1 and c_2 are inverse radii of curvatures, k is the bending rigidity constant, and k_G is the elastic modulus of Gaussian curvature c_1c_2.[19] The parameters k, k_G, and c_0 can be found by analyzing separately the spherical and cylindrical interfaces.[19,21]

Consider a flexible cylinder having the inner radius $R_1 - d$, the outer radius $R_1 + d$ (such that the thickness of the shell is $2d$), and the length l_1, which reshapes into a cylinder having the inner radius $R_2 - d$, the outer radius $R_2 + d$, and the length l_2. This reshaping is equivalent to pure bending if it conserves the membrane area ($R_1l_1 = R_2l_2 = A$). The electric capacitances of these two cylinders are denoted as C_1 and C_2, and further calculations assume constant ΔpH and $d \ll R_1$, R_2. By comparing the difference of electrochemical energy between these two states

$$\Delta W_e = \frac{1}{2}Q^2\frac{C_1 - C_2}{C_1C_2} \approx \frac{d^3(R_1^2 - R_2^2)Q^2}{6\pi\epsilon\epsilon_0 A R_1^2 R_2^2} \tag{12}$$

(at constant electric charge Q) or

$$\Delta W_e = \left\{\frac{1}{2}(\Delta\Psi)^2 - \frac{RT}{F}\Delta\mathrm{pH}\Delta\Psi\right\}(C_2 - C_1) = -\frac{\pi\epsilon\epsilon_0 A d}{3}\frac{(R_2^2 - R_1^2)}{R_1^2 R_2^2}\left\{\frac{1}{2}(\Delta\Psi)^2 - \frac{RT}{F}\Delta\mathrm{pH}\Delta\Psi\right\} \tag{13}$$

(at constant transmembrane potential $\Delta\Psi$) with the difference of surface energy

$$\Delta W_b = \frac{\pi k A(R_2^2 - R_1^2)}{R_1^2 R_2^2} - \frac{2\pi k c_0 A(R_2 - R_1)}{R_1 R_2} \tag{14}$$

one obtains

$$c_0 = 0 \tag{15}$$

and

$$k = \frac{\epsilon\epsilon_0(\Delta\Psi)^2 d}{6} \tag{16}$$

if Q = constant or

$$c_0 = 0 \tag{17}$$

and

$$k = -\frac{\epsilon\epsilon_0 d}{3}\left\{\frac{1}{2}(\Delta\Psi)^2 - \frac{RT}{F}\Delta\mathrm{pH}\Delta\Psi\right\} \tag{18}$$

if $\Delta\Psi$ = constant.

Consider now bending of a cylinder into a sphere, which conserves membrane thickness and total surface area. Performing similar calculations, one obtains

$$k_G = k \tag{19}$$

where k is given by eq 16 in the case of constant Q or by eq 18 in the case of constant $\Delta\Psi$.

With a σ_e estimate of 0.5 or -0.38 mN/m for the corresponding limiting conditions and membrane thickness $2d$ equal to 7 nm,[15] one obtains -4.1×10^{-21} and 3.1×10^{-21} J estimates for the k and k_G at constant $\Delta\Psi$ or Q, respectively.

3. Metabolic Control Over the Inner Mitochondrial Membrane Tension and Bending Elasticity. In this section the characteristic relaxation times of electrical processes within the mitochondria at two different metabolic steady-state conditions (state 3 and state 4) are estimated and compared with the timing of mechanical processes.

Consider the mitochondria as an electric circuit (Figure 2A), which consists of a battery ϵ_E and a resistor r_E representing the respiratory chain, a battery ϵ_P and a resistor r_P representing the phosphorylation system (which incorporates F_0-F_1 ATPase, adenine nucleotide translocator, and inorganic phosphate transporter), membrane capacitance C, and a leak resistor r_L (which includes proton leak itself and cation cycling reactions). For the sake of simplicity, within this model I will neglect the difference between Δp and $\Delta\Psi$. The current I_E generated by the electron transport chain feeds electron flow I_P against potential ϵ_P (giving rise to ATP production), charge accumulation across the membrane dQ/dt, and charge dispersion via leak and ion transport conductances I_L

$$I_E = I_P + \frac{dQ}{dt} + I_L \tag{20}$$

Although some of the r_E, r_P, and r_L parameters are not independent of the proton-motive force (see, for example, ref 22 for the r_L dependence on Δp), these values can still be used for estimation of the relaxation time τ of the electric circuit

$$\tau \approx C r_{E||P||L} \tag{21}$$

where $r_{E||P||L}$ is the equivalent resistance of all resistors connected in parallel calculated at given steady-state conditions. This time constant should be compared with the characteristic frequency ν of the standing waves of contraction and expansion emerging in lipid membranes.[23] Such undulations take place in lipid bilayers and in cell membranes with wavelengths of approximately 100 nm, amplitudes of about 10 nm,[24] and

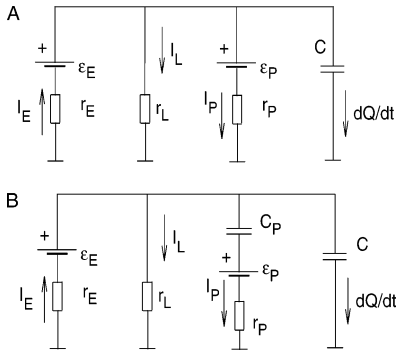

Figure 2. Electric circuit of the inner mitochondrial membrane: (A) the case of the phosphorylation system not being limited by the matrix ADP concentration, state 3 respiration; (B) the case of the phosphorylation system being close to equilibrium, with the matrix ADP concentration limiting and adenine nucleotide exchange and phosphate transport shut down, state 4 respiration.

frequencies about 10 Hz.[23] If $\nu\tau \ll 1$, then the electric relaxation occurs faster than mechanical disturbances change the membrane capacitance so that the membrane behaves as a capacitor at constant voltage applied. In contrast, if $\nu\tau \gg 1$, then membrane deformations do not affect the electric charge of the capacitor.

Estimates for $r_{E||P||L}$ can be obtained from results of so-called top-down experiments on the isolated mitochondria.[25] This analysis allows discrimination of the fluxes through substrate oxidation, phosphorylation, and proton leakage by measuring the respiration rate and Δp at various controlled Δp production and consumption rates. The steady-state values for the total current (which is proportional to the respiration rate) and Δp are

$$\Delta p = \frac{r_L(\epsilon_E r_P + \epsilon_P r_E)}{r_L r_P + r_E r_P + r_L r_E} \tag{22}$$

and

$$I_E = \frac{\epsilon_E r_P + (\epsilon_E - \epsilon_P) r_L}{r_L r_P + r_E r_P + r_L r_E} \tag{23}$$

In the presence of oligomycin, which blocks phosphorylation, these values change to

$$\Delta p_O = \frac{r_L \epsilon_E}{r_L + r_E} \tag{24}$$

and

$$I_{E,O} = \frac{\epsilon_E}{r_E + r_L} \tag{25}$$

The slope of the plot of I_E versus Δp during titration of the phosphorylation subsystem equals

$$\left(\frac{\partial I_E}{\partial \Delta p}\right)_{\epsilon_E, r_E} = -\frac{1}{r_E} \tag{26}$$

while the slope of the $I_E-\Delta p$ plot during titration of the respiration subsystem equals

$$\left(\frac{\partial I_E}{\partial \Delta p}\right)_{\epsilon_P, r_P} = \frac{1}{r_L} + \frac{1}{r_P} \tag{27}$$

These two values are enough to obtain $r_{E||P||L}$. In top-down

analysis, the two components of the electron consumption are discriminated and for our purpose should be recombined. The leak flux measured in the presence of oligomycin has the slope

$$\left(\frac{\partial I_{E,O}}{\partial \Delta p_O}\right)_{\epsilon_P, r_P} = \frac{1}{r_L} \tag{28}$$

Finally, the $I_P-\Delta p$ plot during titration of the respiration subsystem has the slope of

$$\left(\frac{\partial I_P}{\partial \Delta p}\right)_{\epsilon_p, r_p} = \frac{1}{r_P} \tag{29}$$

Thus,

$$\frac{1}{r_{E||P||L}} = -\left(\frac{\partial I_E}{\partial \Delta p}\right)_{E_E, r_E} + \left(\frac{\partial I_{E,O}}{\partial \Delta p_O}\right)_{E_P, r_P} + \left(\frac{\partial I_P}{\partial \Delta p}\right)_{E_P, r_P} \tag{30}$$

According to Figure 5 in ref 26, at 25 °C the proton leakage slope (in the presence of oligomycin) is approximately 0.49 nmol O_2 min^{-1} mg $protein^{-1}$ mV^{-1} at $\Delta p = -180$ mV (which is close to state 4 respiration conditions in this particular study) and negligible at $\Delta p = -135$ mV (state 3 approximation). The slope of I_E versus Δp during titration of the phosphorylation subsystem is approximately -1.12 nmol O_2 min^{-1} mg $protein^{-1}$ mV^{-1}. The value of r_P undergoes dramatic changes upon state 4 to state 3 transition. The slope of the $I_P-\Delta p$ plot during titration of the respiration subsystem is near zero at $\Delta p = -180$ mV and 2.94 nmol O_2 min^{-1} mg $protein^{-1}$ mV^{-1} at $\Delta p = -135$ mV. Thus, $1/r_{E||P||L}$ is about 1.61 nmol O_2 min^{-1} mg $protein^{-1}$ mV^{-1} in state 4 and 4.06 nmol O_2 min^{-1} mg $protein^{-1}$ mV^{-1} in state 3. Using a matrix volume estimate of 1.21 μL mg $protein^{-1}$ for rat liver mitochondria,[26] a membrane capacitance per unit area c of 3 $\mu F/cm^2$, and an average mitochondrial diameter of 0.93 μm (Figure 9 in ref 27, which gives an average mitochondrial volume of a single mitochondria of 4.3×10^{-10} μL) and assuming electron to molecules of oxygen reduced ratio equal to 4, I obtained $r_{E||P||L}$ of 2.5×10^{11} Ω in state 4 and 1.0×10^{11} Ω in state 3.

Consider now the electric capacitance of the mitochondria in state 4 (high substrate and low ADP level). In this state the amount of ADP falls to a level that limits phosphorylation rate.[28] The phosphorylation potential is determined by equilibrium concentrations of adenine nucleotides and phosphate

$$\epsilon_{ATP} = \epsilon_{ATP}{}^0 + \frac{RT}{F} \ln \frac{[ATP]_0}{[ADP]_0[P_i]_0} \tag{31}$$

If the system slightly deviates from equilibrium so that nonzero I_P arises, then the amounts of mitochondrial ADP, ATP, and P_i can be approximated by

$$[ADP] \approx [ADP]_0 - \frac{1}{zVF}\int^t I_P(\tau)\, d\tau \tag{32}$$

$$[ATP] \approx [ATP]_0 + \frac{1}{zVF}\int^t I_P(\tau)\, d\tau \tag{33}$$

$$[P_i] \approx [P_i]_0 - \frac{1}{zVF}\int^t I_P(\tau)\, d\tau \tag{34}$$

where V is the matrix volume of a single mitochondria and z is the number of electrons needed to produce one ATP molecule. ϵ_P can be approximated by ϵ_{ATP}/z so that

$$\epsilon_P \approx \epsilon_P^{Eq} - \frac{RT}{zF}\ln\left\{1 - \frac{1}{FVz[ADP]_0}\int^t I_P(\tau)\, d\tau\right\} + \frac{RT}{zF}\ln\left\{1 + \frac{1}{FVz[ATP]_0}\int^t I_P(\tau)\, d\tau\right\} - \frac{RT}{zF}\ln\left\{1 - \frac{1}{FVz[P_i]_0}\int^t I_P(\tau)\, d\tau\right\} \approx \epsilon_P^{Eq} + \frac{RT}{z^2F^2V}\left(\frac{1}{[ADP]_0} + \frac{1}{[ATP]_0} + \frac{1}{[P_i]_0}\right)\int^t I_P(\tau)\, d\tau \tag{35}$$

This means that under conditions of limited ADP supply ϵ_P will behave toward small disturbances as a constant ϵ_P^{Eq} connected in series with capacitance C_P (Figure 2B)

$$C_P \approx \frac{z^2F^2V}{RT}\left(\frac{1}{[ADP]_0} + \frac{1}{[ATP]_0} + \frac{1}{[P_i]_0}\right)^{-1} \tag{36}$$

As the mitochondrial ADP and ATP concentrations in resting mitochondria are approximately 5 and 15 nmol mg $protein^{-1}$,[29] matrix inorganic phosphate is approximately 2.6 times the cytosolic concentration[30] (giving finally ~4 mM), and $z \approx 3.3$, the effective mitochondrial capacitance $C_P \approx 3.0 \times 10^{-11}$ F in state 4 is by several orders of magnitude higher the real mitochondrial membrane capacitance $C \approx 8.2 \times 10^{-14}$ F.

The obtained estimates $r_{E||P||L}$ of 2.5×10^{11} Ω in state 4 and 1.0×10^{11} Ω in state 3 and effective system capacitances in states 4 and 3 of 3×10^{-11} and 8.2×10^{-14} F, respectively, finally yield $\tau = C_P r_{E||P||L} \approx 7.6$ s in state 4 and $\tau = C r_{E||P||L} \approx 8.2 \times 10^{-3}$ s in state 3. The quantity $\nu\tau$ is on the order of $\sim 10^1 - 10^2 \gg 1$ in state 4 compared to $\sim 10^{-2} - 10^{-1} \ll 1$ in state 3. To summarize, in state 4 the relaxation in the electric circuit occurs much slower than mechanical disturbances of the inner mitochondrial membrane arise, while in state 3 it occurs much faster. Effectively, in state 4 the membrane behaves as an electric capacitor at constant charge, whereas in state 3 it behaves as if constant voltage is maintained. Using the approximate values of the components of Δp in state 3, -135 mV for $\Delta\Psi$ and -35 mV for $(RT/F)\Delta pH$,[22] one obtains the estimates for the elastic parameters of the inner mitochondrial membrane in state 3 as follows: $\sigma_e \approx 0.34$ mN/m and $k = k_G \approx -2.8 \times 10^{-21}$ J.

4. Role of Surface Potential. Internal potentials and surface potentials contribute to the total membrane potential, and the biological effects associated with these components could be significant. The density of fixed charges in biomembranes reaches 10^{-6} C/cm^{-2},[31-33] whereas the density of mobile charges at the inner mitochondrial membrane is only approximately 10^{-7} C/cm^{-2}. However, the screening effect by dissolved ions greatly reduces the electrostatic contribution of fixed surface charges in the surface tension coefficient and bending elasticity parameters. According to eq 7 in ref 34, in the Debye−Huckel approximation if surface charge densities γ_1 and γ_2 at two sides of the membrane are constant during the membrane deformations, then the electromechanical contribution into the surface tension, bending rigidity coefficient, modulus of Gaussian curvature, and spontaneous curvature are

$$\sigma_s = \frac{\gamma^2(1+\delta^2)}{\epsilon_0\epsilon_w\chi} \tag{37}$$

$$k_s = \frac{\gamma^2(1+\delta^2)}{\epsilon_0\epsilon_w\chi}\frac{3}{4\chi^2} \tag{38}$$

$$k_{Gs} = -\frac{\gamma^2(1+\delta^2)}{\epsilon_0\epsilon_w\chi}\left(\frac{1}{2\chi^2}+\frac{d}{4\chi}\right) \quad (39)$$

$$c_{0s} = \delta\frac{4\chi}{3}\frac{(1-2\chi d)}{(1+\delta^2)} \quad (40)$$

where ϵ_w is dielectric constant of water, χ is the inverse Debye length for given ionic solutions, $\gamma = (\gamma_1 + \gamma_2)/2$, and $\delta = (\gamma_2 - \gamma_1)/2\gamma$. (See also ref 35 for the calculation of these parameters at various conditions.) Inserting $\epsilon_w = 80$, $\epsilon_0 = 8.85 \times 10^{-12}$ F/m, $\gamma \approx 10^{-6}$ C/cm^{-2}, $\delta \approx 0$, and $1/\chi \approx 0.8$ nm, one obtains $\sigma_s \approx 0.11$ mN/m. Thus, despite 1 order of magnitude difference in the surface charge densities of fixed and mobile charges, the magnitude of σ_s is several times less than σ_e in state 3 or 4. Moreover, unlike σ_e, σ_s is static as it is much less dependent on metabolic and ionic conditions. Finally, numerical estimations yield $k_s \approx 5.4 \times 10^{-23}$ J and $k_{Gs} \approx -1.2 \times 10^{-22}$ J, which are 1−2 orders of magnitude less than k and k_G. Thus, the protonmotive force is the main electromechanical factor in the inner mitochondrial tension and bending elasticity.

Discussion

This study provides analytical expressions for the surface tension, the bending rigidity constant, and the elastic modulus of Gaussian curvature arising due to modified Coulomb (electrochemical) forces and shows that changes in fluxes within the oxidative phosphorylation system dramatically affect lateral tension and bending elasticity in the inner mitochondrial membrane. In state 4 (high substrate and low ADP levels) the magnitudes of the effective electrochemical surface tension coefficient, bending rigidity constant, and elastic modulus of Gaussian curvature are −0.38 mN/m, 3.1×10^{-21} J, and 3.1×10^{-21} J, respectively. In state 3 (high substrate and high ADP levels) the magnitude of the electrochemical surface tension coefficient increases to 0.34 mN/m, while the bending rigidity constant and the elastic modulus of the Gaussian curvature both decrease to -2.8×10^{-21} J. During a state 4 to state 3 transition the ensuing change of the electromechanical pressure at the cristae junctions (from -2.5×10^4 to 2.2×10^4 Pa) acts toward narrowing the junction necks (Figure 1, black arrows), whereas the decrease in bending rigidity constant promotes membrane folding. At the same time, the decrease in the elastic modulus of Gaussian curvature may lead to an increase in the number of cristae junctions and intertubular junctions within the cristae. According to Gauss−Bonnet theorem, the contribution to the free energy of the membrane's Gaussian curvature integrated over the whole membrane surface equals $2\pi k_G\chi$

$$\oint k_G c_1 c_2 \, dS = 2\pi k_G \chi \quad (41)$$

where χ is the Euler characteristic of the surface. One can assume that narrow cristae junctions and intertubular junctions within the cristae are tightly regulated and heavily supported by structural mitochondrial proteins.[13] This means that the inner mitochondrial membrane at these junctions is more "solid" and less "liquid" than elsewhere. Therefore, during integration of Gaussian curvature over the whole membrane surface, the contribution of such saddle-like (i.e., having negative Gaussian curvature, Figure 1) areas should be "down-weighted" or even omitted. Omitting these junctions will result in integration over a number of unconnected surfaces with an Euler characteristic of approximately 2

$$\oint k_G c_1 c_2 \, dS \approx 4\pi k_G N \quad (42)$$

where N is the number of cristae and intertubular junctions. The decrease in the effective elastic modulus of Gaussian curvature of the inner mitochondrial membrane during state 4 to state 3 transition may therefore be compromised by an increase in the number of junctions within the membrane.

The theory's prediction of a transient contraction and folding of the inner mitochondrial membrane during a state 4 to state 3 transition agrees well with the experiments,[27] in which state 4 to 3 and state 2 to 3 transitions resulted in dramatic condensation of the inner mitochondrial membrane so that it changed from an "orthodox" to a "condensed" conformation. It is worth noting that prolonged exposure of the mitochondria to low substrate and high ADP levels (state 2) reverses F_0-F_1 ATPase so that Δp is maintained at the expense of ATP. In this case, just as in state 4, fluctuations of I_P result in "charging" ϵ_P, i.e., charging the effective capacitance C_P. Thus, the relaxation time in the mitochondrial equivalent electric circuit in state 2 is similar to that in state 4, such that a state 2 to state 3 transition leads to similar membrane remodeling. The theory also predicts an increase in the number of cristae junctions during such remodeling, which has been seen in the experiments.[13] Taken together, the ultrastructural changes in the mitochondria during progression through various respiration states seem to be inline with changes of electromechanical tension and bending elasticity.

The absolute values of σ_e obtained under the two limiting conditions (eqs 7 and 9) are almost 1 order of magnitude higher than the experimentally measured surface tension coefficient $\sigma \approx 0.04-0.05$ mN/m of the plasma membrane in cells kept at normal ambient osmolarity.[36,37] The difference is even higher when σ_e is compared with the surface tension of plasma membrane blebs lacking cortical cytoskeleton support, having $\sigma \approx 0.011-0.012$ mN/m.[38] At the same time, the obtained absolute values of σ_e have the same order of magnitude as the experimentally measured surface tension (0.12−0.4 mN/m) for the plasma membrane in cells subjected to hypotonic stress[36] and are less than the critical membrane tensions of approximately 1−4 mN/m for breaking peptide-free lipid bilayers[39] and 10 mN/m for a breaking cell membrane.[5] The estimated change for the surface pressure P_e by 4.7×10^4 Pa at cristae junctions during a state 4 to state 3 transition is small in terms of osmotic gradients (20 mOsm). However, this pressure is substantial compared with typical intermolecular forces in the membrane. As estimated, the pressure of 2×10^3 Pa can be sufficient for membrane−cytoskeleton disjoining in erythrocytes.[40] Therefore considerable elastic forces provided by mitochondrial structural proteins are essential to counteract P_e at places where the membrane curvature is high. This can explain the remarkable durability of the inner mitochondrial membrane (e.g., compared with the outer membrane) observed during high-amplitude mitochondrial swelling and apoptosis. The estimated electrochemical contribution to the bending rigidity constant and the elastic modulus of Gaussian curvature ($\sim 10^{-21}$ J) is about 1 order of magnitude less than the bending rigidity of biological membranes experimentally measured ($10^{-20}-10^{-19}$ J) [41,42] and can still be of a physiological significance. In contrast to fixed charges, mobile charges do not contribute to spontaneous curvature. However, the numerical estimates for the effects associated with fixed surface charges at the inner mitochondrial membrane ($k_s \approx 5.4 \times 10^{-23}$ J and $k_{Gs} \approx -1.2 \times 10^{-22}$ J) seem to be unimportant for the mitochondria.

In live cells the metabolic conditions of the mitochondria can be between the extremes of state 4 or 3. Thus, in physiological

conditions $\nu\tau$ may be closer to the borderline, which determines whether σ_e is positive or negative. Hence, in reality the magnitudes of σ_e, k, and k_G may be smaller than the estimates obtained in two extreme conditions. Importantly, the membrane tension and bending elasticity can change reversibly and very quickly with changes in metabolic conditions. It has been suggested that low-amplitude changes of the optical density of the mitochondria may reflect structural rearrangements of light-refracting components of the mitochondria rather than changes in total matrix volume.[43] Indeed, during a state 4 to state 3 transition the optical density of the mitochondria increases much faster[44] than when the optical density changes are driven by active water extrusion from the matrix.[43,45] The metabolic regulation of the mechanical properties of the inner mitochondrial membrane described in this study provides the mechanism for the fast structural rearrangements of the membrane. In comparison with it, the osmotic transport acts at a slower time scale but gives rise to larger mechanical forces.[46] The regulation of the macroscopic mechanical parameters of the inner mitochondrial membrane may also act in synergy with the mechanisms of control of mitochondrial topology by membrane-associated macromolecules (reviewed in ref 13). Short incubation with the proapototic protein t-Bid and adenine nucleotide translocator ligands induces morphological changes in the mitochondria, including changes in curvature of the cristae membranes. Mutations in F_0-F_1 ATP synthase and a knockout of mitofilin also affect cristae morphology. Finally, changes in the expression of various mitochondrial GTP-binding proteins involved in fission and fusion processes also profoundly affect the topology of the inner mitochondrial membrane. It is interesting therefore to note that bending properties and surface pressure may theoretically play a part in fusion of the inner membrane. This process is believed to proceed via formation of the intermediate fusion buds, which have high curvature and therefore should be quite sensitive to variations in the mechanical properties of the membrane. Interestingly, dissipation of the proton-motive force blocks fusion of the inner mitochondrial membrane, and this blockage is not mediated by ATP depletion and, hence, probably not by an effect on molecular motors.[47] Thus, metabolic regulation of the macroscopic mechanical parameters of the inner mitochondrial membrane is an important global mechanism of dynamic control of the mitochondrial morphology additional to the control provided by membrane-associated macromolecules.

The fast control over the mechanical properties of the inner mitochondrial membrane can be important for the mitochondrial function. The lateral tension and bending elasticity have been suggested to play a crucial role in the regulation of plasma membrane shape and dynamics.[3−7] The reshaping of the inner mitochondrial membrane due to changes in elastic properties of the inner mitochondrial membrane then can produce a negative feedback to the rate of oxidative phosphorylation. For example, increase in the ADP concentration promotes matrix folding so that a decrease in the diameters of the cristae junctions will reduce the availability of ADP.[16,17] Upon changes in metabolic conditions the relaxation time of the mitochondrial equivalent circuit varies by up to 3 orders of magnitude (from 8.2×10^{-3} to 7.6 s). Meanwhile, the proton-motive force changes not so dramatically (approximately from -230 to -170 mV [22]). This means that the mechanical properties of the inner mitochondrial membrane can be regulated without substantial changes of the mitochondrial membrane potential, i.e., essentially without mitochondrial de-energizing. Interestingly, there are reports of other biological systems in which a change in transmembrane potential alone is sufficient to affect the structure of a biomembrane. In erythrocytes the membrane potential controls extracellular pH-driven membrane reshaping.[48] Measurements using atomic force spectroscopy showed that changing the membrane potential in voltage clamped untransfected HEK293 cells by ± 10 mV altered cell linear size by a few nanometers.[49] Notably, in these examples the electrochemical effects on the membrane elastic properties are expected to be much smaller than those in the mitochondria (because the magnitudes of σ_e, k, and k_G are roughly proportional to the transmembrane potential squared), which highlights the significance of the described phenomenon in relation to the mitochondria.

Conclusions

High transmembrane potential across the inner mitochondrial membrane gives rise to an effective surface tension coefficient of remarkably high magnitude and substantially contributes to the bending rigidity constant and the elastic modulus of Gaussian curvature of the membrane. These values can undergo dramatic variations in time due to changes in the metabolic status of the mitochondria. During a state 4 to state 3 respiration transition the electrochemical contribution in the lateral tension for the inner mitochondrial membrane reverses from -0.38 to 0.34 mN/m, causing a 4.7×10^4 Pa increment in the surface pressure at cristae junctions. At the same time, the electrochemical components of both the bending rigidity constant and the elastic modulus of Gaussian curvature decrease from 3.1×10^{-21} to -2.8×10^{-21} J. Metabolic-dependent changes of elastic properties of the inner mitochondrial membrane can promote mitochondrial remodeling between its principal geometric shapes. These predictions are in good agreement with previous experimental observations of the ultrastructural changes in mitochondria progressing through various respiration states.

Acknowledgment. I thank Ole H. Petersen, Alexei V Tepikin, and Mark Houghton. This work was supported by a Medical Research Council program grant (G880/575).

References and Notes

(1) McMahon, H. T.; Gallop, J. L. Membrane curvature and mechanisms of dynamic cell membrane remodeling. *Nature* **2005**, *438* (7068), 590−596.

(2) Zimmerberg, J.; Kozlov, M. M. How proteins produce cellular membrane curvature. *Nat. Rev. Mol. Cell Biol.* **2005**, *7*, 9−19.

(3) Albrecht-Buehler, G. Role of cortical tension in fibroblast shape and movement. *Cell Motil. Cytoskeleton* **1987**, *7* (1), 54−67.

(4) Bereiter-Hahn, J.; Karl, I.; Luers, H.; Voth, M. Mechanical basis of cell shape: Investigations with the scanning acoustic microscope. *Biochem. Cell Biol.* **1995**, *73* (7−8), 337−348.

(5) Sheetz, M. P.; Dai, J. Modulation of membrane dynamics and cell motility by membrane tension. *Trends Cell Biol.* **1996**, *6* (3), 85−89.

(6) Canham, P. B. The minimum energy of bending as a possible explanation of the biconcave shape of the human red blood cell. *J. Theor. Biol.* **1970**, *26* (1), 61−81.

(7) Fung, Y. C. Theoretical considerations of the elasticity of red cells and small blood vessels. *Fed. Proc.* **1966**, *25* (6), 1761−1772.

(8) McLaughlin, S. The electrostatic properties of membranes. *Annu. Rev. Biophys. Biophys. Chem.* **1989**, *18*, 113−136.

(9) Petrov, A. G.; Bivas, I. Elastic and flexoelectric aspects of out-of-plane fluctuations in biological and model membranes. *Prog. Surf. Sci.* **1984**, *16*, 389−512.

(10) Karbowski, M.; Youle, R. J. Dynamics of mitochondrial morphology in healthy cells and during apoptosis. *Cell Death Differ.* **2003**, *10* (8), 870−880.

(11) Okamoto, K.; Shaw, J. M. Mitochondrial morphology and dynamics in yeast and multicellular eukaryotes. *Annu. Rev. Genet.* **2005**, *39*, 503−536.

(12) Scott, S. V.; Cassidy-Stone, A.; Meeusen, S. L.; Nunnari, J. Staying in aerobic shape: How the structural integrity of mitochondria and mitochondrial DNA is maintained. *Curr. Opin. Cell Biol.* **2003**, *15* (4), 482−488.

(13) Mannella, C. A. Structure and dynamics of the mitochondrial inner membrane cristae. *Biochim. Biophys. Acta* **2006**, *1763* (5−6), 542−548.

(14) Kirichok, Y.; Krapivinsky, G.; Clapham, D. E. The mitochondrial calcium uniporter is a highly selective ion channel. *Nature* **2004**, *427* (6972), 360−364.

(15) Frey, T. G.; Mannella, C. A. The internal structure of mitochondria. *Trends Biochem. Sci.* **2000**, *25* (7), 319−324.

(16) Mannella, C. A.; Pfeiffer, D. R.; Bradshaw, P. C.; Moraru, I. I.; Slepchenko, B.; Loew, L. M.; Hsieh, C. E.; Buttle, K.; Marko, M. Topology of the mitochondrial inner membrane: Dynamics and bioenergetic implications. *IUBMB. Life* **2001**, *52* (3−5), 93−100.

(17) Westerhoff, H. V.; Kell, D. B.; Kamp, F.; Van Dam, K. The membranes involved in proton-mediated free-energy transduction: Thermodynamic implications of their physical structure. In *Microcompartmentation*; Jones, D. P., Ed.; CRC Press: Boca Raton, FL, 1988; pp 115−154.

(18) Evans, E. A. Bending resistance and chemically induced moments in membrane bilayers. *Biophys. J.* **1974**, *14* (12), 923−931.

(19) Helfrich, W. Elastic properties of lipid bilayers: theory and possible experiments. *Z. Naturforsch., C: J. Biosci.* **1973**, *28*, 693−703.

(20) Rand, R.; Burton, A. Mechanical properties of the red cell membrane. I. Membrane stiffness and intracellular pressure. *Biophys. J.* **1964**, *45*, 115−135.

(21) van Giessen, A. E.; van Giessen, A. E.; Blokhuis, E. M.; Blokhuis, E. M.; Bukman, D. J.; Bukman, D. J. Mean field curvature corrections to the surface tension. *J. Chem. Phys.* **1998**, *108* (3), 1148−1156.

(22) Nicholls, D. G. The influence of respiration and ATP hydrolysis on the proton-electrochemical gradient across the inner membrane of rat-liver mitochondria as determined by ion distribution. *Eur. J. Biochem.* **1974**, *50* (1), 305−315.

(23) Larsson, K. On periodic curvature and standing wave motions in cell membranes. *Chem. Phys. Lipids* **1997**, *88* (1), 15−20.

(24) Sackmann, E. Supported membranes: Scientific and practical applications. *Science* **1996**, *271* (5245), 43−48.

(25) Hafner, R. P.; Brown, G. C.; Brand, M. D. Analysis of the control of respiration rate, phosphorylation rate, proton leak rate and protonmotive force in isolated mitochondria using the 'top-down' approach of metabolic control theory. *Eur. J. Biochem.* **1990**, *188* (2), 313−319.

(26) Dufour, S.; Rousse, N.; Canioni, P.; Diolez, P. Top-down control analysis of temperature effect on oxidative phosphorylation. *Biochem. J.* **1996**, *314* (Part 3), 743−751.

(27) Hackenbrock, C. R. Ultrastructural bases for metabolically linked mechanical activity in mitochondria. I. Reversible ultrastructural changes with change in metabolic steady state in isolated liver mitochondria. *J. Cell Biol.* **1966**, *30* (2), 269−297.

(28) Chance, B.; Williams, G. Respiratory enzymes in oxidative phosphorylation. III. The steady state. *J. Biol. Chem.* **1955**, *217* (1), 409−427.

(29) Schild, L.; Blair, P. V.; Davis, W. I.; Baugh, S. Effect of adenine nucleotide pool size in mitochondria on intramitochondrial ATP levels. *Biochim. Biophys. Acta* **1999**, *1413* (1), 14−20.

(30) Garlick, P. B.; Brown, T. R.; Sullivan, R. H.; Ugurbil, K. Observation of a second phosphate pool in the perfused heart by ^{31}P NMR; Is this the mitochondrial phosphate? *J. Mol. Cell. Cardiol.* **1983**, *15* (12), 855−858.

(31) Abramson, H. A.; Moyer, L. S.; Gorin, M. H. *Electrophoresis of Protein and the Chemistry of Cell Surfaces*; Reinhold Publishing Corporation: New York, 1942.

(32) Chiu, V. C.; Mouring, D.; Watson, B. D.; Haynes, D. H. Measurement of surface potential and surface charge densities of sarcoplasmic reticulum membranes. *J. Membr. Biol.* **1980**, *56* (2), 121−132.

(33) Hille, B. Charges and potentials at the nerve surface. Divalent ions and pH. *J. Gen. Physiol* **1968**, *51* (2), 221−236.

(34) Winterhalter, M.; Helfrich, W. Effect of surface charge on the curvature elasticity of membranes. *J. Phys. Chem.* **1988**, *92*, 6865−6867.

(35) Lekkerkerker, H. N. W. The electric contribution to the curvature elastic moduli of charged fluid interfaces. *Physica A* **1990**, *167*, 384−394.

(36) Dai, J.; Sheetz, M. P.; Wan, X.; Morris, C. E. Membrane tension in swelling and shrinking molluscan neurons. *J. Neurosci.* **1998**, *18* (17), 6681−6692.

(37) Derenyi, I.; Julicher, F.; Prost, J. Formation and interaction of membrane tubes. *Phys. Rev. Lett.* **2002**, *88* (23), 238101.

(38) Dai, J.; Sheetz, M. P. Membrane tether formation from blebbing cells. *Biophys. J.* **1999**, *77* (6), 3363−3370.

(39) Leontiadou, H.; Mark, A. E.; Marrink, S. J. Molecular dynamics simulations of hydrophilic pores in lipid bilayers. *Biophys. J.* **2004**, *86* (4), 2156−2164.

(40) Mukhopadhyay, R.; Lim, H. W. G.; Wortis, M. Echinocyte shapes: Bending, stretching, and shear determine spicule shape and spacing. *Biophys. J.* **2002**, *82* (4), 1756−1772.

(41) Beblik, G.; Servuss, R.-M.; Helfrich, W. Bilayer bending rigidity of some synthetic lecithins. *J. Phys.* **1985**, *46*, 1773−1778.

(42) Zilker, A.; Engelhardt, H.; Sackmann, E. Dynamic reflection interference contrast (RIC-) microscopy: a new method to study surface excitations of cells and to measure membrane bending elastic moduli. *J. Phys.* **1987**, *48* (12), 2139−2151.

(43) Lehninger, A. L. Water uptake and extrusion by mitochondria in relation to oxidative phosphorylation. *Physiol Rev.* **1962**, *42*, 467−517.

(44) Packer, L. Size and shape transformations correlated with oxidative phosphorylation in mitochondria. I. Swelling−shrinkage mechanisms in intact mitochondria. *J. Cell Biol.* **1963**, *18*, 487−494.

(45) Azzone, G. F.; Massari, S.; Pozzan, T. Mechanism of active shrinkage in mitochondria II. Coupling between strong electrolyte fluxes. *Biochim. Biophys. Acta* **1976**, *423* (1), 27−41.

(46) Charras, G. T.; Yarrow, J. C.; Horton, M. A.; Mahadevan, L.; Mitchison, T. J. Non-equilibration of hydrostatic pressure in blebbing cells. *Nature* **2005**, *435* (7040), 365−369.

(47) Malka, F.; Guillery, O.; Cifuentes-Diaz, C.; Guillou, E.; Belenguer, P.; Lombes, A.; Rojo, M. Separate fusion of outer and inner mitochondrial membranes. *EMBO Rep.* **2005**, *6* (9), 853−859.

(48) Glaser, R. Does the transmembrane potential ($\Delta\Psi$) or the intracellular pH (pHi) control the shape of human erythrocytes? *Biophys. J.* **1998**, *75* (1), 569−570.

(49) Mosbacher, J.; Langer, M.; Horber, J. K.; Sachs, F. Voltage-dependent membrane displacements measured by atomic force microscopy. *J. Gen. Physiol.* **1998**, *111* (1), 65−74.